Electronic Supplementary Material (ESI) for Chemical Communications
This journal is © The Royal Society of Chemistry 2012
ChemComm

SUPPORTING INFORMATION

Photodynamic Ion Sensor Systems with Spiropyran: Photoactivated Acidity Changes in Plasticized Poly(Vinyl Chloride)

Günter Mistlberger, Gastón A. Crespo, Xiaojiang Xie and Eric Bakker

Chemical structures and Mechanism of the Photoconversion of Spiropyran

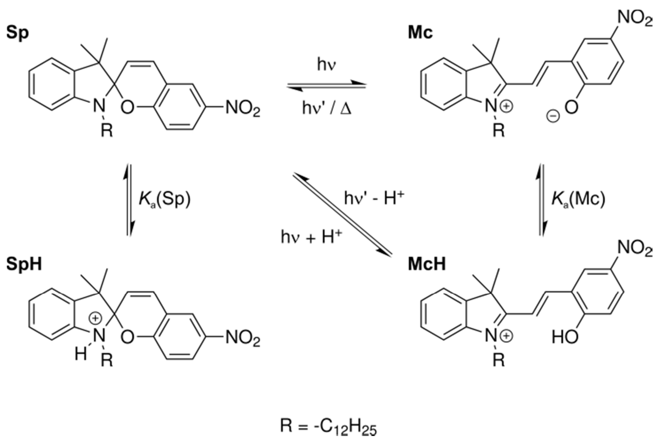

Scheme S1 Structures and mechanisms involved in the photochemical behaviour of 1'-dodecyl-3',3'-dimethyl-6-nitro-spiro[2*H*-1-benzopyran-2,2'-indoline] (Sp).

Absorbance and Luminescence Spectra

Figure S1a shows the absorbance spectra of the dye in basic THF/H_2O (35 µM dye, 50 mM NaOH, THF+H_2O = 20+1) before (Sp) and after (Mc) illumination at 365 nm for one minute. The spectra are consistent with a color change from colorless to purple upon ring opening by UV irradiation (Sp → Mc). Upon addition of hydrochloric acid (100 mM) to the basic solution of Sp the color changes only negligibly (Sp → SpH). However, after switching to the corresponding merocyanine form, the solution turns from colorless to yellow, as evidenced by the strong absorption in the blue region of the spectrum (SpH → McH). Since the pK_a of Sp is expected to be low,[1] it is likely that the band at 430 nm stems from residual McH. While in nonpolar environments and at room temperature the equilibrium between Sp and Mc is on the side of Sp,[2] a fraction will always be in the Mc form. Owing to its increased pK_a, the Mc form protonates quickly in acidic solutions to form McH. McH, on the other hand, is more stable and will hardly transform back to SpH without photochemical stimulation.[3] Consequently, Mc is continuously removed from the Sp/Mc equilibrium in acidic solution and may eventually lead to a McH enriched solution.

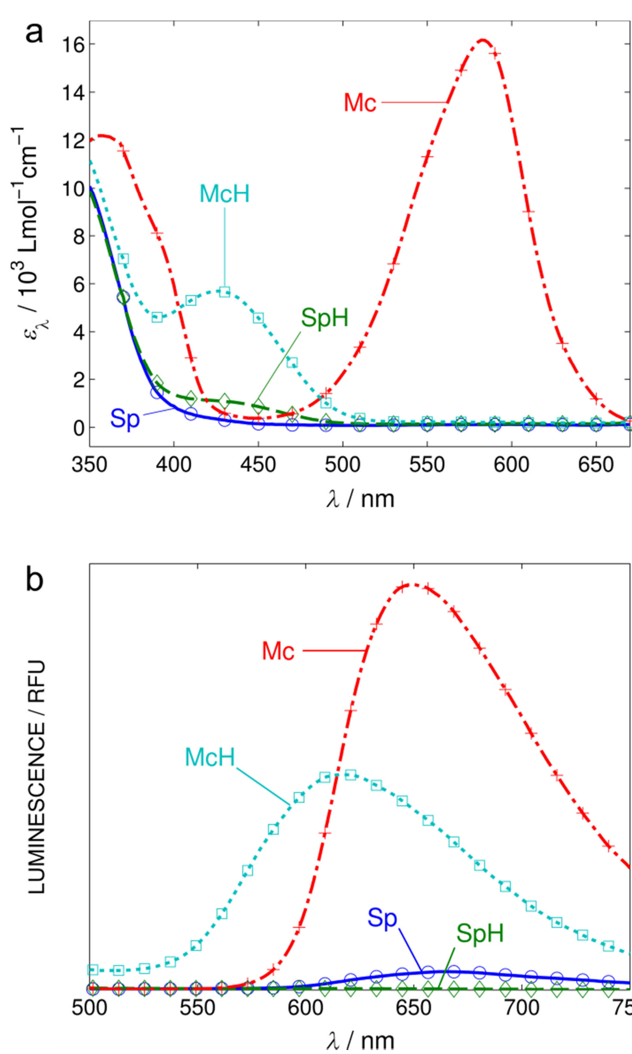

Fig. S1 Spectral properties of Sp, SpH, Mc and McH. (a) Absorbance spectra show the significant change in color from slightly yellow to purple upon switching from Sp to Mc. The yellow color of the McH form is explained by the strong absobance of blue light between 400 and 500 nm. (b) Luminescence spectra show the strong emission of the Mc forms, while the ring closed Sp forms are practically non-luminescent.

Due to fast photo conversion between Mc and Sp upon illumination, fluorescence emission spectra for Sp and Mc had to be recorded at two different excitation wavelengths, i.e. 365 nm for Mc and 410 nm for Sp. The luminescence spectra in Figure S1b clearly demonstrate that the open Mc form is significantly more luminescent than the close Sp form, both protonated and deprotonated. The weak, but still significant luminescence of Sp might even originate from a small fraction of Mc in the Sp solution, which might be formed at a 410 nm excitation. Nevertheless, time trace measurements, where the wavelength was quickly switched from 365 to 410 nm, evidenced the fact that the difference in luminescence intensity is not due to the excitation wavelength. In other words, Mc produced almost the same luminescence intensity when excited at 410 or 365 nm (Figure S2). After illumination of the acidic SpH solution with 365 nm for 2 min, the luminescence significantly increased with a peak at 620 nm (SpH → McH). Addition of triethylamine in excess immediately deprotonated McH to form Mc which showed bright orange/red fluorescence with a maximum at 650 nm. This change in fluorescence properties upon deprotonation (McH → Mc) is very attractive for the application as internal proton indicator after switching the dye to the open Mc form.

Kinetic Aspects and Comparison between Luminescence and Potential Response

While the main aim of this work was to obtain the above mentioned thermodynamic parameters, a comparison of the EMF signal with the luminescence at 650 nm acquired during illumination with 365 and 410 nm, respectively, gives some insight into kinetic processes in the membrane (Figure S2). The pH change from 8 to 3 affected only the potentiometric response and not the luminescence signal. Indeed, concentrations in the membrane phase are negligible in the Nernstian response region of the ion-selective electrodes and no changes in the optical response characteristics are expected.

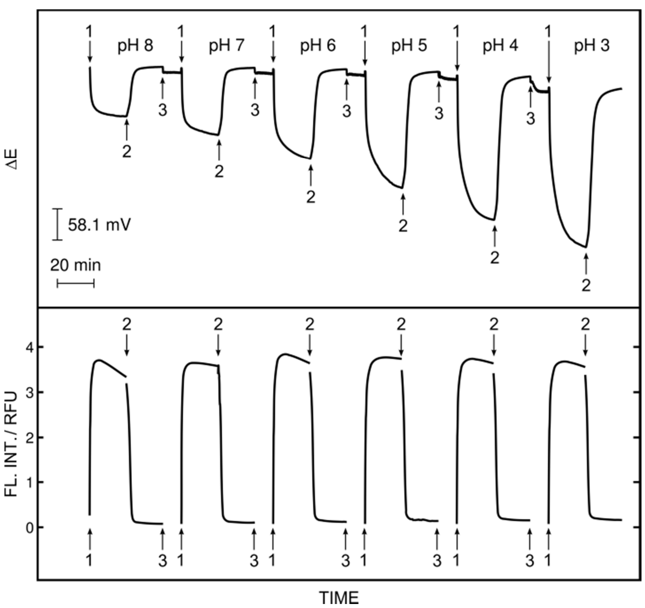

Fig. S2 Comparison of potentiometric response to pH and light with 365 and 410 nm, respectively. with luminescence intensity at 650 nm under the same conditions. Legend: (1): Illumination at 365 nm, (2): 410 nm, (3): light off, flushing with next buffer.

The luminescence signal also seems to indicate the bulk switching efficiency, of the dye from Sp to Mc. Illumination at 365 nm increases the luminescence intensity at 680 nm following roughly saturation kinetics. The slight decrease in signal upon prolonged illumination might be partly because of leaching, bleaching or protonation of the dye. Decomposition of spiropyran upon illumination with UV light can happen because of the formation of reactive singlet oxygen upon quenching of Mc in the excited triplet state.[2] Leaching, on the other hand, can be explained by the decreased log*P* value after ring opening. Even the chinoid form of Mc has a more than three units reduced log*P* value compared to the ring closed spiro form (data calculated using ACDChemSketch). The charged form will certainly increase its water solubility. The third possibility of signal decrease is the protonation of the dye and, consequently, a decreased absorption coefficient at the excitation wavelength and emission quantum yield at 650 nm. The latter point would also explain the almost quantitative recovery after one regeneration cycle. Another possible explanation for the signal recovery is diffusion of dye back into the focus of the optical fiber during relaxation. Illuminating the membrane with 410 nm efficiently triggers the Mc → Sp reaction, diminishing the luminescence with a time t_{90} (time for 90% signal change) of ca. 3 minutes.

The rate of *EMF* change, especially in the Sp → McH reaction at lower pH, is significantly slower than the fluorescence response time and suggests multiple diffusion processes contribute to the signal kinetics. Protonation will mainly happen at the surface, after which McH molecules will continuously diffuse into the membrane bulk. On the other hand, the absorbance measurement across the membranes indicates that more than 99% of the light is absorbed in the membrane bulk, suggesting a significant concentration gradient of the switched species in the membrane. While this is not visible in fluorescence mode, the phase boundary concentrations, and hence the membrane potential, will likely take longer to stabilize.

Reproducibility

The membrane-to-membrane variation of the EMF signal was typically ± 2 mV for the blank membrane and ± 7 mV for the membrane containing spiropyran. This is also evidenced in Figure S3, which shows the potentiometric time response behavior of two membranes for different sample pH values.

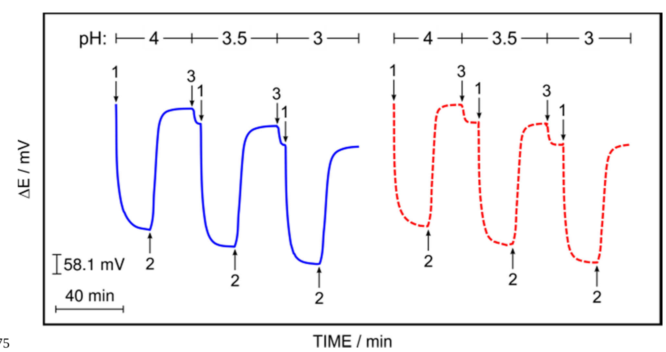

Fig. S3 Repeatability of the potential response to different proton activities in the sample compartment and to irradiation with light of different wavelengths. Legend: (1): Illumination at 365 nm, (2): 410 nm, (3): light off, flushing with next buffer

Materials and Methods

All solvents, salts, acids and bases were of analytical grade and purchased from Sigma. Sodium tetrakis[3,5-bis(trifluoromethyl)-phenyl]borate and bis(2-ethylhexyl) sebacate (DOS) were also from Sigma and used as received. Poly(vinyl chloride) (PVC, high molecular weight) was purchased from Fluka, Switzerland. 1'-dodecyl-3',3'-dimethyl-6-nitro-spiro[2H-1-benzopyran-2,2'-indoline] was synthesized according to Datillo et al.[4]

Absorbance spectra were measured on a Specord 250 absorbance spectrometer (www.analytik-jena.de). Fluorescence spectra were measured on a Fluorolog3 fluorescence spectrometer (www.horiba.com). For combined photoswitching, fluorescence, absorbance and potentiometry experiments a custom made flow cell was produced. The cell allowed reliable mounting of plasticized PVC membranes with 15 to 35 mm diameter. Optical access was granted using quartz windows on both excitation and absorbance side. A bifurcated fiber bundle was attached to the Fluorolog3 spectrometer to project the excitation light of the 450 W short arc xenon lamp onto the membrane. The wavelength was adjusted using the excitation monchromator with a slit width of 10 nm. The luminescence signal was collected and guided to the emission monochromator using the second arm of the fiber bundle (slit width 5 nm). The potential across the membrane was measured using a EMF16 potentiometer (www.lawsonlabs.com) with 10^{15} Ohm input impedence. The electrodes were silver wires coated with AgCl. Transmitted light was monitored with a CCS200 ccd array spectrometer (www.thorlabs.de). Solution exchange in sample and reference compartment was established using a peristaltic pump (Minipuls 3, www.gilson.com).

Membrane preparation

PVC (200 mg), DOS (400 mg), sodium tetrakis[3,5-bis(trifluoromethyl)phenyl]borate (0.53 mg, 1 mmol kg^{-1}) and 1'-dodecyl-3',3'-dimethyl-6-nitro-spiro[2H-1-benzo-pyran-2,2'-indoline] (5.7 mg, 20 mmol kg^{-1}) were dissolved in 3 mL tetrahydrofuran. 1 mL of this cocktail was pipetted into a glass ring (inner diameter 22 mm) fixed to a glass plate and left overnight for evaporation of the solvent. Blank membranes were prepared without spiropyran, but otherwise the same.

Correction of EMF Signals

The electromotive force (EMF) acquired employing the separate solution method was corrected for the change in chloride concentration at the Ag/AgCl element using the following equation:

$$E_{\mathrm{corr}} = E_{\mathrm{exp}} + \frac{2.303RT}{F}\log a_{\mathrm{Cl}}$$

where R, T and F have their established meanings and a_{Cl} is the activity of the indicated species in the aqueous phase. The activity coefficients were calculated using the Debye-Hückel approximation.

Final equation for the formation constant

$$\beta_{\mathrm{JI}} = \frac{K^{\mathrm{pot}}_{\mathrm{TEA,J}}(\mathrm{L})\left[K^{\mathrm{pot}}_{\mathrm{TEA,J}}(\mathrm{L}) - K^{\mathrm{pot}}_{\mathrm{TEA,J}}(\mathrm{R})\right]}{K^{\mathrm{pot}}_{\mathrm{TEA,J}}(\mathrm{R})\left\{\left[K^{\mathrm{pot}}_{\mathrm{TEA,J}}(\mathrm{R}) - K^{\mathrm{pot}}_{\mathrm{TEA,J}}(\mathrm{L})\right]R_{\mathrm{T}} + K^{\mathrm{pot}}_{\mathrm{TEA,J}}(\mathrm{L})L_{\mathrm{T}}\right\}}$$

References for the Supporting Information

1. A. V. Chernyshev, M. S. Chernov'yants, E. N. Voloshina and N. A. Voloshin, *Russ. J. Gen. Chem.*, 2002, **72**, 1468-1472.
2. V. I. Minkin, *Chem. Rev.*, 2004, **104**, 2751-2776.
3. T. Satoh, K. Sumaru, T. Takagi, K. Takai and T. Kanamori, *Phys. Chem. Chem. Phys.*, 2011, **13**, 7322-7329.
4. D. Dattilo, L. Armelao, G. Fois, G. Mistura and M. Maggini, *Langmuir*, 2007, **23**, 12945-12950.